Journal of Electrical Engineering, Electronics, Control and Computer Science – JEEECCS, Volume 9, Issue 34, pages 13-24, 2023

Dynamic Modeling for Hybrid Electric Vehicles with its Performance Optimization Using Different Control Strategies and Energy Management Systems

Shannmukha Naga Raju Vonteddu,
Department of EEE,
UCEK, JNTUK, Kakinada, India.
raj.shanmukha@gmail.com

Ravindra Kollu,
Department of EEE,
UCEK, JNTUK, Kakinada, India
ravikollu@jntucek.ac.in

Prasanthi Kumari Nunna,
School of Engineering,
Department of EEE,
UPES,Dehradun, India.
prasanti@ddn.upes.ac.in

Abstract **– Fuel cell vehicles are one of the main alternatives to conventional vehicles, as new technologies make them more commercially viable. In this context, this work presents some energy management strategies applicable to fuel cell hybrid electric vehicles based on a dynamic model, which allows the performance evaluation and comparison with vehicles powered by internal combustion engines. The model includes a fuel cell stack, batteries, an induction motor and vehicle mechanics. The driver's reactions are monitored by a PI controller, the electric motor is controlled by a slip mode algorithm, and power management is performed subject to constraints such as fuel cell efficiency and battery charge level. Energy consumption is comparable to similar light vehicles with internal combustion engines. The results demonstrate the lower fuel consumption of the fuel cell vehicle and the better performance of the hybrid architecture compared to conventional vehicles. In addition, they confirm the usefulness of the model for simulating hybrid electric vehicles and explore different control strategies to obtain better performance.**

Keywords- Hybrid vehicles; fuel cell; power management; equivalent consumption minimization strategy; Dynamic modelling; slip mode algorithm

I. Introduction

The number of vehicles on the streets of the world is today the largest in history. Of these, most are still propelled by engines that burn fossil fuels, which contribute heavily to the more than 36 x 109 tons of carbon dioxide that are dumped into the atmosphere annually [1]. In this way, the search for solutions to preserve the planet Earth for future generations necessarily involves the design of vehicles that favor the reduction of atmospheric pollution. In this context, vehicles propelled by sustainable energy sources are the central theme. Not by chance, the main manufacturers in the world have been researching and developing vehicles that use alternative energy sources and several countries have already announced goals to reduce the problem: Germany has committed to banishing vehicles powered by fossil fuels by 2030, England will stop the sale of new vehicles powered by oil derivatives from 2040 and, in Norway and India, only fully electric vehicles will be marketed from 2015 and 2030, respectively.

The search for sustainable energy sources to equip land vehicles has led researchers to investigate everything from solar energy and compressed gases to fuels based on algae and alcohol. Among the emerging technologies are electric vehicles [2] and those powered by hydrogen. The main car manufacturers already have commercial versions of vehicles of this type, although their establishment as a real successor to the current ones and their use on a large scale still require a lot of research and development. This work presents some energy management strategies applicable to fuel cell hybrid electric vehicles based on a dynamic model, which allows the performance evaluation and comparison with vehicles powered by internal combustion engines. The model includes a fuel cell stack, batteries, an induction motor and vehicle mechanics.

In addition to vehicles with a single alternative energy source, a recurrent and useful composition is the use of more than one source in the same vehicle. In this case, they are called hybrids 0(HEVs), and are classified into three categories according to their architecture [3], [4], [5]: In the series configuration, the traction force that reaches the wheels is transmitted by one or more electric motors. In the parallel configuration, the vehicle can be propelled directly by the internal combustion engine, through a gear system and/or through electric motors powered by another source(s). In the split configuration, each of the car's axles is powered by a different power source.

Another widespread classification divides HEVs into load maintainers or depletors. The first ones are capable of keeping the battery charge within determined limits in any driving situation, and the others do not have this capacity and need to be connected to the electrical network periodically to recharge the battery.

The use of different energy sources in the same car requires a power management strategy that divides the power demand between the sources and gives the vehicle adequate performance [6], [7]. The power management strategy can be performed using different approaches, grouped into three categories, namely: Heuristic techniques; Static optimization methods and Dynamic optimization methods. Heuristic techniques are well explored in the literature [8], [9], [10] and have in their favor the ease and low cost of implementation, although they generally do not fully explore complex vehicles. In static optimization methods the electrical power is translated into an equivalent amount of steady state fuel consumption to calculate the total cost. An optimal control strategy then determines the appropriate division of the power demand between each of the sources, using efficiency maps. Therefore, they are methods of instantaneous optimization according to the system variables at each instant of time.

The most widespread method of this class is called Equivalent Consumption Minimization Strategy (ECMS). An example of application of this technique in a HEV propelled by an internal combustion engine (ICE) and a Battery Bank (BB) can be found in [11]. The dynamic optimization methods consider the dynamics of the system and the optimization starts to be considered according to a time horizon, instead of specific instants. Although it has global optimization capability, these methods have the disadvantages of being dependent on the driving cycle and cannot be implemented in real time. An application example is found in [12] and [13], where the energy management for a hybrid truck with parallel configuration is done.

Through the literature review it is possible to outline the state of the subject, as well as define the most effective energy management system for an urban residential scenario. A model is sought that is capable of managing the power flow between the home and the network more efficiently, preventing the addition of new load profiles, such as EVs, from overloading the network and also reducing costs with electricity, without affecting the household consumption pattern. This work presents a vision of the current electric power system (EPS), guiding us to the future EPS integrated with energy management systems, its potentials, challenges and limitations, in the direction of a Smart Grid.

Although there has been a surge in the study of energy management strategies in recent years to ensure the effective and sustainable functioning of power sources, the development of energy management strategies is still a crucial topic in FCEV. The strategies that have been described have not undergone a thorough development, but there are strategies that have concentrated on calculating the power of each source while taking a variety of factors into account, such as lifetime, incoming stress, power source efficiency, and so on. Our most recent understanding indicates that in many EMSs, battery SOC zone selection is determined empirically and that efficiency plays no part in this. Additionally, by comparing real-time situations with driving cycles, driving conditions have been identified, and oscillations in FC power can be effectively controlled.

II. LITERATURE REVIEW

The use of different energy sources in the same vehicle demands a control strategy that manages the operation of these systems for better performance. An algorithm that determines the amount of power required for a driver request, as well as the appropriate division of this power between the system's energy sources implements what is defined as a Power Management Strategy, which can be performed by different approaches, grouped into three categories: Heuristic techniques; Static optimization methods and Dynamic optimization methods.

Heuristic techniques such as fuzzy logic and rule-based control for power management of HEVs are well explored in the literature [14-15] and have in their favor the ease and the low cost of implementation, although they generally do not fully exploit complex vehicles. The criteria for defining the rules are usually determined intuitively or based on the designer's experience, and prior knowledge of the conduction cycle to be performed is not necessary, which allows real-time implementation [16].

In static optimization methods the electrical power is translated into an equivalent amount of steady state fuel consumption to calculate the total cost. An optimal control strategy then determines the appropriate split of the power demand between each of the energy sources using efficiency maps. They are, therefore, methods of instantaneous optimization according to the system variables at each instant of time, and can be applied in real time. The most widespread method of this class is called Equivalent Consumption Minimization Strategy (ECMS), initially introduced by [17], at the time applied to a hybrid vehicle propelled by a diesel engine. internal combustion (ICM) in conjunction with a BB, and later explored by other authors, in variations that include the adaptability of the algorithm, so that it estimates the equivalent consumption for a section of the current driving cycle in real time, applying it to the section following [18].

The dynamic optimization methods consider the dynamics of the system and the optimization starts to be treated in according to a time horizon, rather than specific instants. Although they have global optimization capability, these methods have the disadvantage of depending on the conduction cycle and cannot be implemented in real time, being generally used as a comparison parameter for determining the optimality of real-time algorithms [19].

III. ELECTRIC POWER SYSTEM

Electric energy is an indispensable input for the socioeconomic development of all nations. It is through electric energy that it becomes possible to guarantee the maintenance of several essential systems, such as: health, security, education, telecommunications, lighting, agricultural, industrial systems, among many others.

Therefore, countries with large territorial extensions, such as India, have very extensive and complex electrical power systems. According to survey in its monthly operating plan for 2022, generation in India is divided into: hydroelectric (62.5%), wind (11.9%), thermoelectric gas and liquefied natural gas (LNG)) (8.8%), biomass (8.3%), solar (2.7%) oil and diesel thermoelectric (2.5%), coal thermoelectric (1.7%), nuclear (1.1%) and other sources (0.4%).

The complexity of electrical power systems can be seen, especially due to their size, varied sources of generation and seasonality of generation and load. Controlling the power flow in the SEP is a task that requires constant monitoring and more intelligent systems for contingencies, which guides us towards Intelligent Networks, the Smart Grids (SGs).

A. Smart Networks

An electrical grid that employs monitoring, control, communication, self-adaptive intelligence and minimizes costs while increasing security, resilience, flexibility and stability to automatically manage the flow of energy from generation sources to demand, is called Smart Grid [20]. It is possible to evaluate a comparison between the conventional grid and the Smart Grid, shown in Table I.

Table I. COMPARISON BETWEEN THE CONVENTIONAL GRID AND A SMART GRID.

Conventional Network	**Smart Grid**
Unidirectional Meter	Bidirectional Meter
Centralized Generation	Distributed Generation
Supervised	Smart
Blackouts	Adaptive
Few Sensors	Many Sensors

Thus, it is noted that the SG appears as an improvement to the traditional centralized and unidirectional model, but also as a response to the increase in new technologies that will directly affect the electrical networks, such as: distributed generation (DG), electric vehicles, systems storage systems (SAEs), among others that arise [21].

B. Energy Management System

The energy management system is an element that makes up the Smart Grids, coordinating generation with consumption by managing the power flow with specific purposes for each case. A review of the literature on this topic is presented here, seeking to show in general the main uses of an EMS, directing it towards a specific objective.

From [22] and [23], there are the different classifications of EMSs, in this work, however, those based on the role and functions of operation will be presented. Therefore, the following roles of an EMS stand out: minimization of operating costs, minimization of polluting emissions, improvement of voltage stability, improvement of stability and minimization of recovery time, improvement in efficiency.

In minimizing operating costs [24-26], EMS optimizes, based on demand, generation avoiding expensive sources, especially at peak times, combined with a reconfiguration of the distribution system schedule, enabling the reduction of operating costs. In addition, the inclusion of Distributed Generation (DG) comes in as a way to reduce losses with power transmission over long distances, but its integration and operation are in charge of the EMS.

Global warming is one of the world's main concerns, and factors such as vehicle gas consumption and other emissions from fossil fuels are the most harmful. In minimizing polluting emissions [27-28], the EMS plays a role mainly in the choice of sources and distribution of energy, prioritizing renewable means, such as wind, photovoltaic and geothermal generation, reducing gas emissions related to energy demand.

In the role of improving efficiency [29], the EMS assists in monitoring distributed energy, and through IoT technologies, the consumer has his system optimized by scheduling devices that demand energy. Still, through monitoring and control, it is possible to manage energy sources, reducing stress on the network, power losses and consequently increasing the efficiency of the system. For example, in the case of a residence, with DG, EV and loads, adjustments could be made to the sources and loads, leaving the charging of the electric vehicle for the early morning period, when the demand is reduced, even using the battery of the EV as a source of energy at peak times, among other arrangements that improve the efficiency of the house and consequently of the distribution network.

The most used functions, in these cases, are: monitoring, optimization, estimation and forecasting, control and management. Among these, the highest average percentages of energy savings are: control (30%), optimization (25.6%) and management (25%). Still, the best combination of functions in EMS is control/optimization, with an average saving of 21.27%, and the lowest estimation/prediction, with 10% energy saving [22]. In general, the optimization function can be seen as strategies and systems that provide the best schedule of energy use inside the building, making smart decisions, examples are found in [30]. The control function, on the other hand, is seen as strategies and systems that control the operations of devices that consume energy, instead of using an on/off type control, a network was used. neural network in a predictive way, reducing energy consumption by about 20%.

IV. FUEL CELL ELECTRIC VEHICLE MODEL

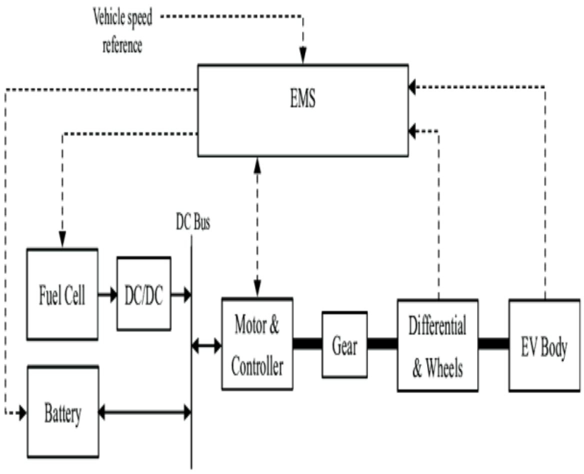

Figure 1. Structure of FCEV

A. Battery pack

Batteries are systems that convert chemical energy into electrical energy. In rechargeable batteries, it is possible to reverse the chemical reaction by reversing the electrical current, and bring the state of charge (SOC) of the battery back to a certain value. A set of batteries is called a battery bank, and is an important component in many electric vehicles, since, in addition to composing the power generation system, it allows the use of braking energy, which in typical urban areas corresponds to more than 25 % of the total traction energy, reaching values around 70% in large cities.

From a specified discharge time (t) and nominal capacity (C), the actual discharge time of a battery can be calculated as a function of the drained current based on a reference load capacity, called Peukert Capacity , defined by Equation (1), in which I_{bat} denotes the current requested from the battery and k is a constant called Peukert coefficient.:

$$C_p = (I_{bat})^k \times t = \left(\frac{C}{t}\right)^k \times t \tag{1}$$

Considering a time interval δt in which a constant current, , I_{bat} , is requested from the battery, the charge removed from it is calculated by Equation (2) (Larminie& Lowry, 2012).

$$Q_{\delta t} = \delta t \times (I_{bat})^k \tag{2}$$

If δt is given in seconds, the total charge removed from the battery after n times of time, Qn, in Ah, is given by Equation (3).

$$Q_n = Q_{n-1} + \frac{\delta t \times (I_{bat})^k}{3600} \tag{3}$$

It is a discrete integrator. In continuous time, with $\delta t \rightarrow 0$, this relationship can be rewritten as shown in Equation (4) which, therefore, describes the amount of charge (energy) that is removed from the battery in a given time interval.

$$Q(t) = \frac{1}{3600}\int_{t_1}^{t_2} (I_{bat})^k \, dt \tag{4}$$

Considering the ratio between this energy and the original battery charge capacity, the state of charge is found by subtracting this value from the initial state (100%), as shown in Equation (5).

$$\begin{aligned} SOC &= 1 - \frac{1}{3600}\int_{t_1}^{t_2} \frac{(I_{bat})^k}{C_p} \, dt \\ &= 1 - \frac{1}{3600}\int_{t_1}^{t_2} \frac{I_{bat}(t)}{C_p} \, dt \end{aligned} \tag{5}$$

The open-circuit voltage (E) depends on the SOC and the number of cells that form the battery, being calculated using Equation (6).

$$E = n \times [2 + 0.15(SOC)] \tag{6}$$

Finally, the voltage between the battery terminals can be determined using Ohm's law, as shown in Equation (7), in which R_{int} is the internal resistance, considered constant as a function of the battery capacity, and calculated with based on the current that would completely discharge it in the course of 10 hours if it were applied constantly over time (I_{10}), as shown in Equation (7).

$$V = E - R_{int} I = E - n \times \frac{0.022}{I_{10}} I \tag{7}$$

B. Fuel cell stack

Like batteries, fuel cells (CaCs) are devices that convert chemical energy into electrical energy. However, unlike batteries, in which the maximum available energy is determined by the amount of stored reagents, a CaC is an energy converter source that can, theoretically, provide electrical energy for as long as fuel is supplied. For this, a gaseous fuel (generally hydrogen) is constantly supplied to the anode (negative electrode) and an oxidant (oxygen) to the cathode (positive electrode). The hydrogen is oxidized at the cathode, resulting in an electron that is conducted through the external circuit, which can feed a charge, and a proton that is conducted through the electrolyte. The process produces electricity, water and heat. The output voltage of a CaC can be defined as:

$$V_{FC} = E_{ocv} - V_{act} - V_{ohmic} - V_{con} \tag{8}$$

Where E_{ocv} is the open circuit voltage (thermodynamic potential) of the cell, V_{act} is the activation loss of the anode and cathode, V_{ohmic} is the ohmic loss and V_{con} the loss resulting from mass transport. The thermodynamic potential is a function of the temperature and partial pressures of oxygen and hydrogen in the cell inlet channels, values that should not vary between cells of the same cell. E_{nerst} is defined by the following equation:

$$\mathrm{E_{ocv}} = \frac{\Delta \mathrm{G}}{2\times \mathrm{F}} + \frac{\Delta \mathrm{S}}{2\times \mathrm{F}} \times (\mathrm{T} - \mathrm{T_{ref}}) + \frac{\mathrm{R}\times\mathrm{T}}{2\times\mathrm{F}} \times \left[\ln\left(\mathrm{P_{H_2}}\right) + \frac{1}{2} \times \ln\left(\mathrm{P_{O_2}}\right)\right] \quad (9)$$

Here, ΔG represents the change in Gibbs free energy, in J/mol, F is the Faraday constant (96.487 C), ΔS is the entropy change (J/mol), R is the universal gas constant (8.314 J/K×mol), P_{O_2} and P_{H_2} the partial pressures of oxygen and hydrogen (atm), respectively, T the operating temperature of the fuel cell and T_{ref} the reference temperature (25°C). In Equation (8), V_{act} is the result of the slowness of the reactions that occur on the surface of the electrodes, in which a part of the generated voltage is used to conduct the chemical reaction that transfers the electrons between the electrodes. This loss is calculated using Equation (10).

$$\mathrm{V_{act}} = -\varepsilon_1 - \mathrm{T}(\varepsilon_2 + \varepsilon_3 \ln \mathrm{C_{O_2}} + \varepsilon_1 \ln \mathrm{i_{FC}} \quad (10)$$

Where $C02$ is the oxygen concentration at the cathode catalytic interface (mol/cm), determined by Equation (11), i_{FC} is the electric current flowing through the CaC, and £i are defined parameterization coefficients based on theoretical equations that take into account thermodynamic, kinetic and electrochemical factors.

$$\mathrm{C_{O_2}} = \frac{\mathrm{P_{O_2}}}{5.08\times10^{6}\times \mathrm{e}^{-498/\mathrm{T}}} \quad (11)$$

The ohmic loss, V_{ohmic} , is due to the resistance to electron transport from the cathode to the anode, being directly proportional to the electric current. It is one of the main sources of energy loss in fuel cells. It is calculated by Equation (12), in which R_M and R_C are the equivalent resistances of the membrane and the resistance to the transfer of protons through it, respectively, A_{fc} is the CaC area, ρ_M is the membrane resistivity and L its thickness.

$$\mathrm{V_{ohmic}} = \mathrm{i_{FC}} \times (\mathrm{R_M} + \mathrm{R_C}) = \mathrm{i_{FC}} \times \quad (12)$$

While A_{fc} and L are measurable dimensional parameters, ρ_M is a function of membrane type and humidity, operating temperature and current density. Membrane resistivity is calculated according to Equation (13) [38] for a Nafion-type membrane, widely used in polymeric membrane cells.

$$\rho_\mathrm{M} = \frac{1+0.03\left(\frac{\mathrm{i_{FC}}}{\mathrm{A_{fc}}}\right)+\left(\frac{\mathrm{T}}{4887.0968}\right)^2\left(\frac{\mathrm{i_{FC}}}{\mathrm{A_{fc}}}\right)^{2.5}}{0.0055\left[\varphi-0.634-3\left(\frac{\mathrm{i_{FC}}}{\mathrm{A_{fc}}}\right)\right]^{\mathrm{e}^{\left[\frac{\mathrm{T}-303}{0.2392\mathrm{T}}\right]}}} \quad (13)$$

Where $0.0055(f - 0.634)$ is the specific membrane resistivity ($\Omega.\ cm$) at 30^oC with i_{FC} = 0. The exponential term in the denominator is the temperature correction for cases where the CaC temperature is not 30^oC. T is the absolute temperature of the cell (K). The term in square brackets in the numerator, together with the term $3i_{FC}\ /A_{fc}$ in the denominator are determined empirically, and represent the correction for the specific resistivity of the membrane as a function of the electric current density and the temperature of the CaC. Parameter f is adjustable depending on the preparation of the membrane and its humidification, among other factors. Still referring to Equation (8), V_{con} is the result of reducing the concentration of oxygen and/or hydrogen at the cathode and anode and is defined by the following equation:

$$\mathrm{V_{con}} = \mathrm{B} \times \ln\left(1 - \frac{\mathrm{J}}{\mathrm{J_{max}}}\right) \quad (14)$$

Where B (Volts) is a parameterization coefficient that depends on the cell and its operating state, and the J_{max} represent the current and current limit densities, in mA/cm².

1) Dynamics of the CaC

The amount of reactions that occur at the electrode/electrolyte interface of a fuel cell depends on the density of electrons and hydrogen ions on the surfaces of both. The greater the charge concentration, the greater the current generated. This charge concentration generates an electrical voltage at the interface and behaves similarly to an electrical capacitor. When the current changes value, sometime is required for the amount of charge stored in the electrode/electrolyte interface to dissipate or increase, that is, the activation voltage does not immediately follow the current as it does with the ohmic voltage. This delay can be equated as follows,

$$\frac{\mathrm{dV_d}}{\mathrm{dt}} = \frac{\mathrm{i_{FC}}}{\mathrm{C}} - \frac{\mathrm{V_d}}{\tau} \quad (15)$$

Where V_d represents the dynamic voltage of the fuel cell, equivalent to the voltage across an electrical capacitance C, with a time constant r, defined according to Equation (16).

$$\tau = \mathrm{c} \times \mathrm{R_a} = \mathrm{C} \times \left(\frac{\mathrm{V_{act}}+\mathrm{V_{con}}}{\mathrm{i_{FC}}}\right) \quad (16)$$

In Equation (16), R_a is the equivalent resistance and the sum $V_{act} + V_{con}$is equal to V_d in Equation (15). Thus, a CaC can be modeled as an electrical circuit according to Figure 2. A computational model to represent the behavior of a fuel cell stack is easily built using Equations (8) to (16), which allow the calculation, from a demanded current, of the battery output voltage and power and of the partial pressures of the gases in the anode and cathode.

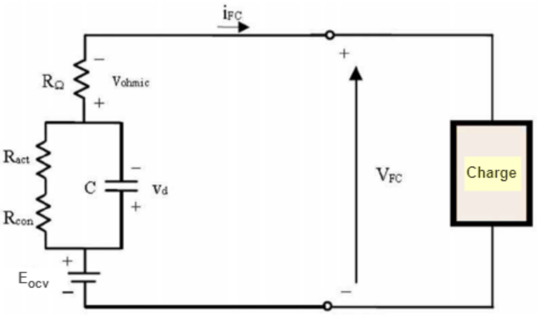

Figure 2. Equivalent electrical circuit of a Fuel Cell.

The voltage and power of the CaCs stack, $V_{Battery}$ and $P_{Battery}$, are found by multiplying the voltage (VF) and power ($PCaC$) of a cell by the number of cells that comprise it (n):

$$V_{Battery} = n \times V_{FC} \quad (17)$$

$$P_{Battery} = n \times V_{FC} \times i_{FC} \quad (18)$$

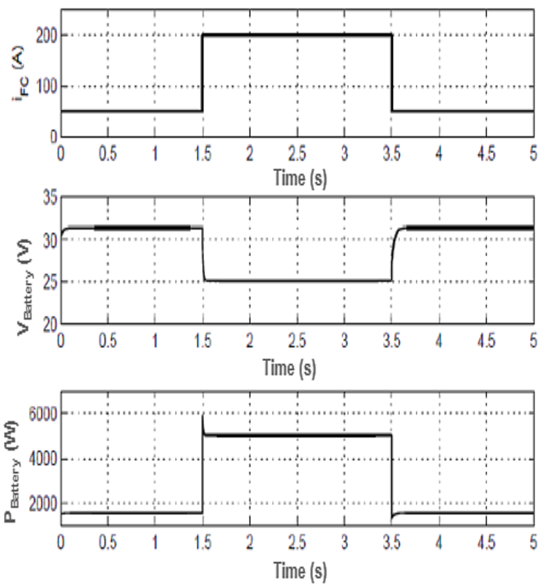

Figure 3. CaC voltage and power as a function of load insertion and removal.

Figure 3 shows the result of the simulation carried out for a stack of polymeric membrane (PEM) CaCs. Although the time constant associated with the variation of the CaCs stack voltage is small, it is possible to notice that the voltage varies more smoothly compared to the current variation.

The electric motor that powers an EPS system might be located in the steering column or mounted directly to the steering gear. Electronic sensors measure how much steering power is needed on various terrains, lessening the strain and effort it takes for the driver to turn the steering wheel.

2) Consumption

The flow rate of consumed hydrogen is calculated as a function of the molar mass (M_{H_2}, in g/mol) of the gas and the electric current passing through the cell (i_{FC}), according to Equation (19).

$$\frac{dm_{H_2}}{dt} = \frac{M_{H_2} i_{FC}}{2F} = 1.05 \times 10^{-8} \times \frac{P_{CaC}}{V_{FC}} \quad (19)$$

Where F is the Faraday constant. Similarly, the consumed Oxygen flow and the produced water flow are calculated according to Equations (20) and (21).

$$\frac{dm_{ar}}{dt} = 3.57 \times 10^{-7} \times \lambda \times \frac{P_{CaC}}{V_{FC}} \quad (20)$$

$$\frac{dm_{H_2O}}{dt} = 9.34 \times 10^{-8} \times \frac{P_{CaC}}{V_{FC}} \quad (21)$$

In Equation (20), λ is the stoichiometric ratio (here considered equal to 2). To find the consumption of a pile of CaCs, instead of a single cell, just multiply Equations (19), (20) and (21) by the number of cells in the pile.

3) Efficiency

The efficiency of a CaC (5) can be determined through Equation (22), where μf is the fuel utilization coefficient [39]

$$\eta_{FC} = \mu_f \times \frac{V_{FC}}{1.48} \times 100\% \quad (22)$$

4) Electric motor

The dynamic model used to represent the behavior of the HEV induction electric motor. The dynamic equations that define it, presented in coordinates (α, β), are shown below:

$$\frac{di_\alpha}{dt} = \beta\eta\varphi_\alpha + \beta\omega\varphi_\beta - \gamma i_\alpha + \frac{1}{\sigma L_S} u_\alpha$$

$$\frac{di_\beta}{dt} = \beta\eta\varphi_\beta + \beta\omega\varphi_\alpha - \gamma i_\beta + \frac{1}{\sigma L_S} u_\beta$$

$$\frac{d\varphi_\alpha}{dt} = -\eta\varphi_\alpha + \omega\varphi_\beta + \eta L_h i_\alpha$$

$$\frac{d\varphi_\beta}{dt} = -\eta\varphi_\beta + \omega\varphi_\alpha + \eta L_h i_\beta$$

$$T = \frac{3N_r L_h}{2L_r}(i_\beta\varphi_\alpha - i_\alpha\varphi_\beta)$$

$$\frac{d\omega}{dt} = \frac{1}{J}(T - T_l) \quad (23)$$

in which:

$$\eta = \frac{R_r}{L_r};\ \beta = \frac{L_r}{\sigma L_S L_r}$$

$$\sigma = 1 - \frac{L_h^2}{L_S L_r};\ \gamma = \frac{R_S + \frac{L_h^2}{L_r} R_r}{\sigma L_S} \quad (24)$$

From the above equations i_α , i_β are the components of the current in the stator at coordinates (α,β), $f\alpha$,$f\beta$ are the components of the magnetic flux in the rotor at coordinates (α,β), u_α , u_β are the components of the voltage in the stator at coordinates (α,β), L_r , L_S, L_h are the rotor, stator and mutual inductances, respectively, R_r, R_S are the rotor and stator resistances, ω = rotor angular speed, J is the rotor moment of inertia of the motor, T is the torque of the motor, T_l is the load torque and N_r is the number of pole pairs.

From the control point of view, the objective is to make the motor follow a reference torque. In other words, the power demanded from the vehicle by the driver is translated into a torque demand from the electric motor which, in order to generate the desired torque, will need to supply power (electric current) from the system's energy sources. The vehicle controller (power management system) will then determine how much power should be required from each source.

The current is obtained through Equation (25).

$$i = \sqrt{i_\alpha^2 + i_\beta^2} \quad (25)$$

The electrical and mechanical powers of the electric motor are calculated according to Equations (26) and (27), respectively, where u is the electrical voltage supplied to the motor.

$$P_{el} = u \times i \quad (26)$$

$$P_{mec} = T \times \omega \quad (27)$$

Consider the following error equations (Yan, et al., 2004):

$$S_T = T - T^* \quad (28)$$

$$S_\varphi = c(\varphi - \varphi^*) + (\dot{\varphi} - \dot{\varphi}^*) \quad (29)$$

S can be found via Equation (23), and can be written as.

$$S = \begin{bmatrix} S_T \\ S_\varphi \end{bmatrix};\ D = \begin{bmatrix} -\varphi_\beta \varphi_\alpha \\ \dfrac{\varphi_\alpha \qquad \varphi_\beta}{\sqrt{\varphi_\alpha^2+\varphi_\beta^2}\sqrt{\varphi_\alpha^2+\varphi_\beta^2}} \end{bmatrix} \quad (30)$$

Where c_1 is constant and f_1 is a continuous function of state variables, both of which are assumed to be bounded. One can determine sliding modes by using the non-linear transformation.

5) Vehicle dynamics

The input signal for the vehicle dynamics is the torque coming from the electric motor and the output signal is the vehicle speed, which is fed back and controlled according to the driver's request, according to Equation (31).

$$\frac{dv}{dt} = \frac{1}{M}\left(\frac{\tau_{ref} - \tau_b}{r_{rad}} - \frac{Bv}{r_{rad}^2} - F_r - F_a\right) \quad (31)$$

in which τ_{ref} is the torque generated by the electric motor (reference torque), τ_b is the friction torque applied to the vehicle wheels, B is the viscous damping coefficient, r_{rad} is the radius of the wheels, M the mass and v the speed of the vehicle, F_r is the rolling resistance force and F_a is the movement resistance force due to aerodynamic drag. The forces F_r and F_a are given by Equations (32) and (33), respectively, where C_d is the aerodynamic drag coefficient, ρ_a the air density, A the frontal area of the vehicle, $C_{rollres}$ the rolling resistance coefficient force normal to the tires.

$$F_r = C_{rollres} \times F_n \quad (32)$$

$$F_a = \frac{1}{2} C_d \rho_a A v^2 \quad (33)$$

The parameters used in the simulations are shown in Table 2 and were mostly taken from the files of the ADVISOR program, a vehicle simulation program developed by the US Department of Energy (DOE) recognized as one of the main car simulators in existence. The mass of the vehicle, originally 825kg, was increased by 140kg to include the average weight of two people. Furthermore, additional mass was used for the different types of VECaCs depending on the approximate weight of the energy sources. In Table II, represents Vehicle parameters.

TABLE II. VEHICLE PARAMETERS.

Parameter	Value	Parameter	Value
M	965 to 1205kg	B	0.001
A	2.332m^2	J_r	41.04 r_{rad}^2
C_d	0.37	g	9.81m/s^2
r_{rad}	0.2711m	ρ_a	1.2kg/m^3
$C_{rollres}$	0.009	F_n	M × g

C. Driver Representation

The driver is the one who imposes the speed to the vehicle by acting on the accelerator and brake pedals. It closes the feedback loop, measuring vehicle speed and comparing it to a reference speed. This behavior can be modeled by a proportional and integral (PI) controller that will act through the reference torque signal for the electric motor. The transfer function of the PI controller is given by Equation (35), where Kp represents the proportional gain and Ti the integral time.

V. POWER MANAGEMENT STRATEGY

VECaCs can be classified into three categories: non-hybrids, non-regenerating hybrids and regenerative hybrids. In regenerative hybrid VECaCs, BB allows some of the energy that would be wasted during braking to be used. In non-hybrid VECaCs there is no regeneration, and the energy generated during braking is wasted through friction brakes or resistor banks. In this configuration, the power request made to the CaCs stack follows the driver's request (except during braking), which may imply frequent operation of the stack in regions of low efficiency due to the high power demand. In the hybrid configuration without regeneration, the energy storage system is used only to support the fuel cell, supplying part of the power to the vehicle when it operates in regions of low efficiency. In these VECas, the BB can be recharged only through the CaCs stack. The advantages of this configuration are its low cost and the simplicity of its power electronics.

A. *Driving cycles*

The driving cycle desired by the driver can be emulated through standardized cycles that reproduce different driving situations. In this work, three different cycles were considered, namely: Federal Urban Driving Schedule (FUDS), Highway Fuel Economy Driving Schedule (HFET) and US06 Supplemental Federal Test Procedure (SFTP), all of these established by the North American environmental protection agency (EPA).

The FUDS cycle represents driving conditions in cities, with low speeds and many acceleration and braking situations; HFET stands for road driving, where fairly constant speed is maintained and few acceleration and braking situations are required; and the SFTP cycle simulates an aggressive driving profile, with high speed and acceleration, rapid gear changes and post-start driving conditions. The main characteristics of the three cycles are presented in Table 3.

TABLE III. MAIN CHARACTERISTICS OF CONDUCTION CYCLES.

Cycle	FUDS	HFET	SFTP
Distance (km)	11.8	16.5	12.8
Duration (s)	1372	766	601
Average speed (km/h)	31.4	77.6	77.1
Maximum speed (km/h)	91.2	96.4	129.2
Number of stops	18	1	8

Vehicle control can be summarized as follows:

I. The target speed is compared with the current vehicle speed;
II. The PI controller generates a reference signal that represents the torque required for the vehicle to reach the established speed;
III. The vehicle controller evaluates the required torque and generates a reference signal for the electric motor;
IV. The electric motor controller makes it generate the desired torque;
V. The power required for the electric motor is requested from the energy sources by the vehicle controller. The division of this request is made according to the control strategy and the applicable restrictions.

The reference signal (torque) transmitted to the electric motor may not match the driver's request. It may vary according to the capacity of the electric motor to generate it and the capacity of the energy sources to provide the necessary power. In addition to the power to carry out the driving cycle, the vehicle sources must also be capable of supplying auxiliary systems such as air conditioning, radio, electric windows, interior lighting, etc. In the results that follow, a power of 2kW was added at each instant of time in order to represent the average power demand of the auxiliary systems of a light vehicle.

B. *Non-hybrid VECaC*

The control strategy for non-hybrid fuel cell vehicles is restricted to adjusting the power of the CaC stack to satisfy the load request over time. During braking, the battery is disconnected. Figure 4 presents an example of the results obtained for the FUDS conduction cycle. In this one, $Vveiculo$ is the speed performed by the vehicle, $Pmotor$ is the power required by the induction motor so that it satisfies the driver's request and supplying the auxiliary systems, and $PCaC$ is the power requested from the fuel cell stack. From now on, $Pmotor$ will be treated, for simplicity, as being the request for power by the driver of the vehicle.

Table 3 presents the amount of hydrogen consumed and the average efficiency of the CaC stack over the FUDS, HFET and SFTP cycles. The HFET cycle implies the lowest consumption of hydrogen, as the power needed to carry it out is lower than the other two. The SFTP and FUDS cycles, on the other hand, result in practically the same consumption. As there is no auxiliary energy source, the CaCs stack operates with low efficiency in many moments.

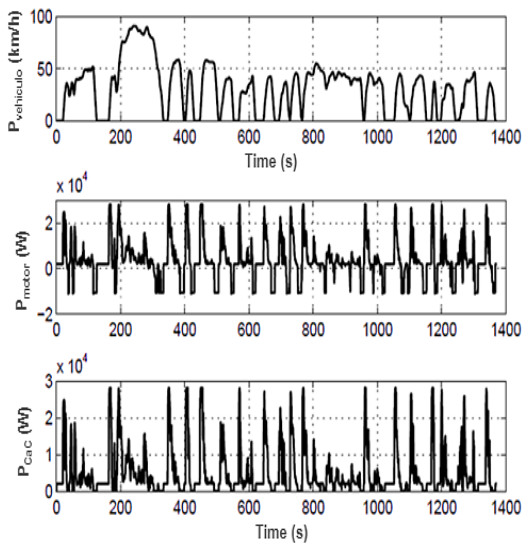

Figure 4. Non-hybrid VECaC with FUDS cycle.

TABLE IV. CONSUMPTION AND YFC FOR THE NON-HYBRID VECAC.

Cycle	η_{FC}	SOC average
FUDS	12.90×10^{-2}	47.83%
HFET	10.23×10^{-2}	42.62%
SFTP	12.33×10^{-2}	43.19%

C. Hybrid VECaC without regeneration

For hybrid VECaCs without regeneration, the controller must trigger the battery bank so that it supplies part of the energy when the CaCs stack operates with low efficiency or when the power demand is very high. In this case, the power of the cell stack is kept constant and the difference between the driver's request and the power supplied by the cell will be supplied by the battery bank. The strategy is carried out in this way until the BB reaches a minimum charge state limit ($SOCmin$). From this moment on, the battery bank will no longer be used to prevent operation of the CaCs stack in regions of low efficiency until it is charged again, reaching a determined upper limit ($SOCmax$). To this end, the CaCs stack charges the BB at times when the power request is less than the maximum power that the stack is capable of providing.

There may be times when the power requested by the driver is greater than what the CaCs stack is capable of providing. In this condition there are two possible alternatives: Supply the power requested by the driver by activating the BB or supply only the maximum power that the CaCs stack can supply and not activate the battery bank, avoiding discharging it. If the first alternative is used, the useful life of the battery bank will be reduced due to the increase in cycles of use compared to the second option, however there will be times when the vehicle's performance will be compromised due to the power provided by the energy sources be less than the required power. Similarly, it may happen that the SOC of the battery bank reaches the minimum allowed limit and the driver's power request is greater than the CaCs stack is capable of providing. In this case, one must choose between discharging the battery bank beyond the desired limit ($SOCmin$) or maintaining the state of charge at this limit, which implies not satisfying the driver's request. In this work, the BB is used in situations where the power demand is greater than the CaCs stack is capable of providing.

Figure 5 presents the power distribution when the control strategy is applied to perform the FUDS conduction cycle. The maximum power of the CaCs stack is limited to avoid operation in low efficiency regions. A threshold of approximately 30% was used as the minimum allowable efficiency value. The number of cells in the CaC stack was reduced by half compared to the non-hybrid VECaC and the battery bank is made up of 12 Volt, lead-acid batteries (6 cells), similar to those used today in conventional light vehicles.

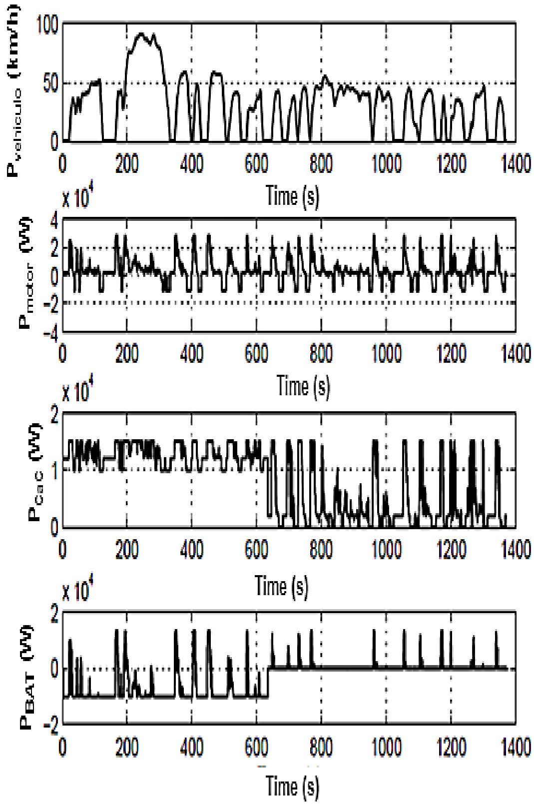

Figure 5. Hybrid Vecac Without Regeneration With FUDS Cycle.

The state of charge of the battery bank for the same simulation is shown in Figure 6. It is observed that the BB stops being charged when it reaches 60% of its capacity. In this simulation, the initial state of charge of the battery bank was fixed at 50%, which is the lower limit of the allowed range ($SOCmin$).The control strategy was also employed considering different driving cycles. Table 5 summarizes the main results achieved.

TABLE V. CONSUMPTION, 5FC AND SOC FOR THE HYBRID VECAC WITHOUT REGENERATION.

Cycle	η_{FC}	SOC average
FUDS	12.90×10^{-2}	47.83%
HFET	10.23×10^{-2}	42.62%
SFTP	12.33×10^{-2}	43.19%

It can be seen that the average efficiency of the CaC stack, although still less than 50%, is higher than that of the non-hybrid VECaC for the three conduction cycles. This value is not even higher, because the CaCs stack is frequently used to charge the BB, which makes it constantly operate with efficiency close to the minimum allowed value. However, with the insertion of BB, the consumption of hydrogen decreased in relation to the non-hybrid VECaC.

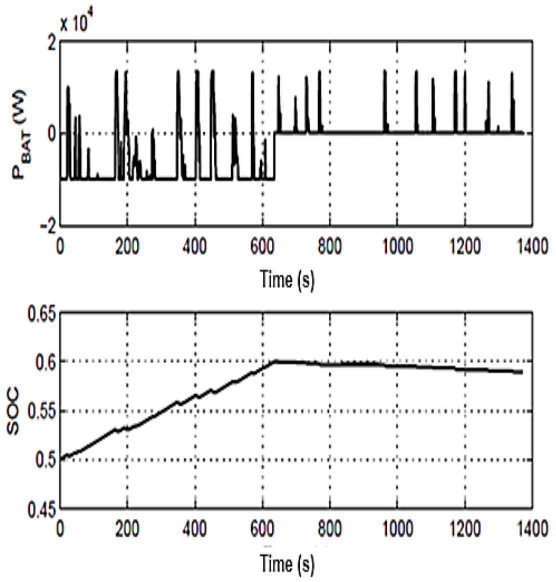

Figure 6. SOC of hybrid VECaC without regeneration with FUDS cycle.

D. VECaC regenerative hybrid

In this configuration, the control algorithm aims to take advantage of energy from braking and keep the SOC of the battery bank as close as possible to a predetermined ideal value (SOCi). To this end, in addition to avoiding the operation of the CaCs stack in regions of low efficiency, and controlling the SOC of the BB between established limits, the controller penalizes the SOC depending on the difference between its current value and the SOCi. In this way, the deterioration imposed on the battery due to high charge and discharge currents is minimized. The algorithm operates the vehicle in two distinct modes: Fast charging and normal charging.

Fast recharge mode prevents the BB from having its state of charge diminished beyond $SOCmin$. In this mode, the CaCs stack continuously delivers its maximum power until the SOC reaches the predetermined ideal value. In this study, the SOCideal is fixed at 55%, which is the average value of the allowed range. In replay mode ga normal, the power requested from the CaCs stack is controlled between the minimum ($Pmin$) and maximum values. In addition, the SOC of the battery bank is maintained between $SOCmin$ and $SOCmax$ and have their fluctuation in relation to SOCideal by increasing or decreasing the power request made to the BB. The normal recharge mode can be described through four different stages, namely:

• **Regeneration**: The power supply from the CaCs stack is interrupted and the BB is charged through regenerative braking. When SOC = 0, regeneration is stopped.

• **Low Power:** Prevents operation of the CaCs stack in regions of low efficiency. When little power is demanded to the vehicle, the battery is disconnected and the BB supplies the necessary power.

• **High Power:** The CaCs stack provides its maximum power while the BB provides the necessary additional power.

• **Moderate Power:** When the SOC of the battery bank is above the ideal value, the BB is discharged proportionally the difference between the SOC and the SOCideal, as shown in Equation (34).

Also Additional power is provided by the CaCs stack. When the SOC is below the ideal SOC, the CaCs stack provides the power to propel the vehicle and an additional one to charge the BB. This additional is calculated according to Equation (35).

$$P_{bat} = \left(P_{motor} - P_{CaC_{max}}\right) \times \varphi \qquad (34)$$

$$P_{bat} = -P_{motor} \times \varphi \qquad (35)$$

in which:

$$\varphi = \frac{\frac{SOC_{max}+SOC_{min}}{2} - SOC}{\frac{SOC_{max}-SOC_{min}}{2}} \qquad (36)$$

In Figure 7, the vehicle speed and the powers requested from each of the sources can be observed so that it performs the FUDS driving cycle using the control strategy described in this section. The initial SOC of the battery bank was fixed at 50%. Figure 7 shows the state of charge of the BB for the same situation.

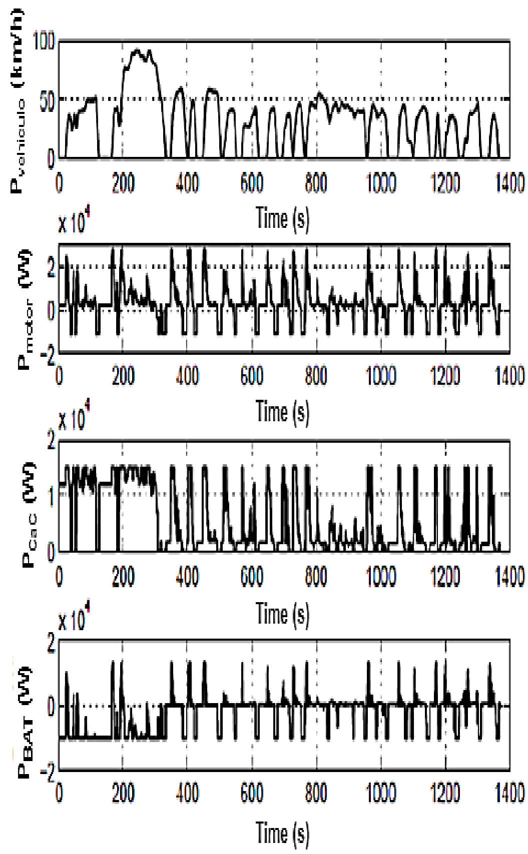

Figure 7. Regenerative hybrid VECaC for the FUDS cycle.

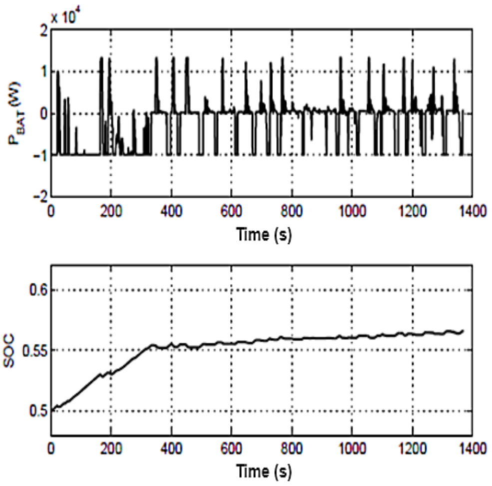

Figure 8. SOC of regenerative hybrid VECaC for FUDS cycle.

The system starts its operation in fast recharge mode, since the initial SOC of the BB is the minimum allowed limit. Operation is maintained in this mode for approximately 340s, the time required for the BB to reach 55% of its charge (SOCi). At that moment, the operation switches to normal charging mode, which means that the CaCs stack is no longer used to charge the battery. It is charged at the instants in which the induction motor operates as a generator from the mechanical braking energy. Table 6 presents the results obtained for the FUDS, HFET and SFTP conduction cycles.

TABLE VI. CONSUMPTION, YFC AND SOC FOR THE HYBRID REGENERATIVE VECAC

Cycle	Consumption of $H_2(kg)$	η_{FC}	SOC averag e
FUDS	07.94×10^{-2}	55.89%	55.29%
HFET	04.79×10^{-2}	55.37%	53.86%
SFTP	08.35×10^{-2}	47.08%	54.55%

E. Comparison with conventional vehicles

To compare the consumption of VECaCs with that of light vehicles powered by an internal combustion engine, an equivalent consumption of gasoline can be calculated, which represents the mass of hydrogen consumed plus the battery energy consumed by the VECaC.

Table 6 presents the equivalent average consumption for the configurations of VECaCs treated in this work, compared to the average consumption of a conventional light vehicle powered exclusively by an ICE for three driving cycles. The simulation of the consumption of conventional vehicles is not part of the scope of this work, however a comparison in order of magnitude is useful to guide the performance of the different configurations of VECaCs proposed here. Thus, the values presented in Table 7 for the fuel consumption of light passenger vehicles propelled by ICE are the same for all driving cycles, being used only as a reference to give an idea of the potential for improvement achievable by the VECaCs.

TABLE VII. EQUIVALENT CONSUMPTION IN KM/L OF GASOLINE.

Vehicle	FUDS	HFET	SFTP
Vehicle 1.0 Conventional	12.00	12.00	12.00
non-hybrid VECaC	25.45	62.49	36.65
Hybrid VECaC without regeneration	39.07	63.35	34.02
Regenerative hybrid VECaC	39.43	65.95	43.23

The dependence of vehicle consumption on the driving cycle performed is evident. Driving the vehicle on the road (HFET cycle) implies lower consumption than driving in the city (FUDS) and/or aggressive driving (SFTP). In all cases, however, the consumption of the hybrid vehicle decreased in relation to the non-hybrid. In addition to the lower cost associated with battery power, the insertion of regenerative capacity has proven to be a way to reduce consumption. It can be seen that the improvement is more pronounced in the hybrid VECaC compared to the non-hybrid for the FUDS and SFTP cycles, in which there is a greater amount of regeneration energy.

VI. CONCLUSION

A literature review allows finding the main references of works related to electric energy management systems, some with a broader scope, and others more particular, but all of them demonstrate that the implementation of energy management techniques leads to benefits when consuming and /or for the distribution network, mainly on network efficiency, reduction of peak demand and reduction of energy costs. Furthermore, it is evidenced that the control/optimization type management systems are the ones that result in greater energy savings, with an average reduction of 21.27% in the consumption of electric energy. Therefore, the search for references of this topology should generate better results in energy management works. In addition, this work presents a dynamic model for fuel cell hybrid electric vehicles and applicable strategies for power management between their energy sources. A computational model is detailed, which allows evaluating the behavior of such vehicles according to different power requests. The model consists of a battery bank, a fuel cell stack and an electric motor, as well as a PI controller that represents the driver's reactions, a sliding mode controller for the electric motor and a controller for power management.

The computational implementation is presented according to parameters that represent a light passenger vehicle, allowing the comparison of energy consumption of hybrid vehicles with vehicles of similar size equipped with internal combustion engines. Three configurations are evaluated: non-hybrid VECaC, hybrid non-regenerating VECaC, regenerative hybrid VECaC. The results prove the improvement in the fuel consumption of the VECaCs in relation to conventional ICE vehicles and demonstrate the better performance (lower consumption) of the hybrid vehicles. The developed model can be easily adapted to different types of vehicles and serve as a basis for carrying out more complex studies, such as the insertion of the dynamics of other subsystems (power systems, auxiliary instruments, among others), the use of other sources of energy generation and/or storage (super capacitors, hydraulic systems, etc.) and the development of new control strategies.

CONFLICTS OF INTEREST:

On behalf of all authors, the corresponding author states that there is no conflict of interest.

REFERENCES:

[1] AL-Ghaili. A. M. et al. “Energy Management Systems and Strategies in Buildings Sector: A scoping Review,” IEEE Access, vol. 9, pp. 63790-63813, 2021.

[2] Alam, M. S. Arefifar S. A. “Energy Management in Power Distribution Systems: Review, Classification, Limitations and Challenges,” IEEE Access, vol. 7, pp. 92979-93001, 2019.

[3] Aneel.Agência Nacionalde Energiaelétrica - Aneel.[S.l.], . Disponível em:[https://www.aneel.gov.br/], 2022.

[4] Zhang, S., Yang, L., Zhao, X., Qiang, J. “A GA optimization for lithium-ion battery equalization based on SOC estimation by NN and FLC”. Int. J. Electr. Power Energy Syst. 73, 318e328. 2021.

[5] R. Venkatasatish, C. Dhanamjayulu, “Reinforcement learning based energy management systems and hydrogen refuelling stations for fuel cell electric vehicles: An overview”, International Journal of Hydrogen Energy”, Volume 47, Issue 64, Pages 27646-27670, 2022.

[6] K. Gautam, M. Tariq, J. P. Pandey, K. S. Verma and S. Urooj, "Hybrid sources powered electric vehicle configuration and integrated optimal power management strategy," in IEEE Access, vol. 10, pp. 121684-121711, 2022.

[7] Xu, X. Guo and Q. Xun, "Loss minimization based energy management for a dual motor electric vehicle," 2022 IEEE Transportation Electrification Conference and Expo, Asia-Pacific (ITEC Asia-Pacific), Haining, China, pp.1-6, 2022.[IEEE Transportation Electrification Conference and Expo, Asia-Pacific (ITEC Asia-Pacific), China, 2022].

[8] Y. Lu, S. Liu, M. Wu and D. Kong, "Energy management of dual energy sources pure electric vehicle based on fuzzy control," IEEE International Conference on Internet of Things and Intelligence Systems (IoTaIS), Bandung, Indonesia, 2021, pp. 228-233, [International Conference on Internet of Things and Intelligence Systems (IoTaIS), Indonesia,2021].

[9] Saeed Zeynali, Naghi Rostami, Ali Ahmadian, Ali Elkamel, , “Stochastic energy management of an electricity retailer with a novel plug-in electric vehicle-based demand response program and energy storage system: A linearized battery degradation cost model”, Sustainable Cities and Society, Volume 74, 103154, ISSN 2210-6707. 2021.

[10] Ping Li, Xiaohong Jiao, Yang Li, “Adaptive real-time energy management control strategy based on fuzzy inference system for plug-in hybrid electric vehicles”, Control Engineering Practice, Volume 107, 104703, ISSN 0967-0661.2021.

[11] Amoroso, M. M. Wireless Networking Technologies For Smart Homes: A Technical And Economic Analysis, 2020.

[12] Divshali, P. H.; Choi, B. J.; Liang, H. “Multi-agent Transactive Energy management system considering high levels of renewable energy source and electric vehicles”. IET Generation, Transmission & Distribution, vol.11,no. 15, pp. 3713-3721, 2017.

[13] Han, J. et al. “Smart home energy management system including renewable energy based on ZigBee and PLC,” IEEE Trans. Consum. Electron., vol. 60, no. 2, pp. 198-202, 2014.

[14] International Energy Agency (IEA) World Energy Outlook 2020.

[15] Jayachandran, M. et al. “Operational planning steps in smart electric power delivery system”. Scientific Reports, NatureResearch,v. 11, 12 2021.ISSN 20452322. 2021.

[16] Shima Nazari; Francesco Borrelli;Anna Stefanopoulou, “Electric Vehicles for Smart Buildings: A Survey on Applications, Energy Management Methods, and Battery Degradation” Proceedings of the IEEE, Vol. 109, No. 6, pp. 1128 – 1144, 2021.

[17] Yuying Hu; Cailian Chen; Tian He;Jianping He; Xinping Guan;Bo Yang, “Proactive power management scheme for hybrid electric storage system in evs: an mpc method” IEEE Transactions on Intelligent Transportation Systems, Vol. 21, No. 12, pp. 5246 – 5257, 2020.

[18] Kannayeram, N.B. Prakash, R. Muniraj, “Intelligent hybrid controller for power flow management of PV/battery/FC/SC system in smart grid applications,” International Journal of Hydrogen Energy, Volume 45, Issue 41, pp. 21779-21795, 2021.

[19] Junjie Hu;Huayanran Zhou;Yang Li;Peng Hou;Guangya Yang, “Multi-time scale energy management strategy of aggregator characterized by photovoltaic generation and electric vehicles” Journal of Modern Power Systems and Clean Energy, Vol. 8, No. 4, 2020.

[20] Macarulla M. et al. “Implementation of predictive control in a commercial building energy management system using neural networks”. Energy Buildings, vol. 151, pp. 511-519, 2017.

[21] Mandelman, M. Critical Analysis of the Brazilian energy matrix and the implementation of Smart Grid. 2020.

[22] Marzband, M. et al. “A real-time evaluation of energy management systems for smart hybrid home microgrids”. Electric Power Systems Research 143, ElsevierLtd, pp. 624–633, 2017.

[23] Marzband, M. et al. “An Optimal Energy Management System for Islanded Microgrids Based on Multiperiod Artificial Bee Colony Combined With Markov Chain”. IEEE Systems Journal, vol. 11, no. 3, pp. 1712-1722, Sept. 2017.

[24] Rafique, S. et al. “Energy management systems for residential buildings with electric vehicles and distributed energy resources”. IEEE Access, v.9, pp. 46997–47007, 2021.

[25] Sausen, J. P. et al. “ Analysis of electric vehicle insertion on distribution transformer load curve”. Institute of Electrical and Electronics Engineers, 2017.

[26] Sausen, J. P. et al. “Economic feasibility study of using an electric vehicle and photovoltaic micro generation in a smart home”. IEEE Latin America Transactions, v. 16, pp. 1907–1913, 2018.

[27] Taha,M.S.;Abdeltawab,H.H.;Mohamed,Y.A.I.”An online energy management system for a grid-connected hybrid energy source”. IEEE Journal of Emerging and Selected Topics in Power Electronics, vol. 6,no.4, pp. 2015-2030, Dec.2018.

[28] Wang, Z.; Chen, B.; Wang J.; Kim, J. “Decentralized energy management system for networked microgrids in grid-connected and islanded modes,” IEEE Transactions on Smart Grid, vol. 7, no. 2, pp. 1097-1105, March 2016.

[29] Yue, J. et al. “Optimization scheduling in intelligent energy management system for the dc residential distribution system,” IEEE Second International Conference on DC Microgrids(ICDCM),Nuremburg, pp. 558-563, 2017.[IEEE Second International Conference on DC Microgrids(ICDCM),Nuremburg, 2017].

[30] Zanetta, L. C. Fundamentos de Sistemas Elétricos de Potência. [S.l.]: Editora Livraria daFísica, 2005.